Influence of silicon dangling bonds on germanium thermal diffusion within SiO_2 glass

D. Barba,[1] R. S. Cai,[2] J. Demarche,[3] Y. Q. Wang,[2] G. Terwagne,[3] F. Rosei,[1,4] F. Martin,[1] and G. G. Ross[1]

[1]*INRS Centre for Energy, Materials and Telecommunications, 1650 Boul. Lionel-Boulet, Varennes, Québec J3X 1S2, Canada*
[2]*The Cultivation Base for State Key Laboratory, Qingdao University, Qingdao 266071, People's Republic of China*
[3]*LARN, Centre de Recherche en Physique de la Matière et du Rayonnement (PMR), University of Namur (FUNDP), B-5000 Namur, Belgium*
[4]*Center for Self-Assembled Chemical Structures, McGill University, Montreal, Quebec H3A 2K6, Canada*

(Received 11 February 2014; accepted 28 February 2014; published online 17 March 2014)

We study the influence of silicon dangling bonds on germanium thermal diffusion within silicon oxide and fused silica substrates heated to high temperatures. By using scanning electron microscopy and Rutherford backscattering spectroscopy, we determine that the lower mobility of Ge found within SiO_2/Si films can be associated with the presence of unsaturated SiO_x chemical bonds. Comparative measurements obtained by x-ray photoelectron spectroscopy show that 10% of silicon dangling bonds can reduce Ge desorption by 80%. Thus, the decrease of the silicon oxidation state yields a greater thermal stability of Ge inside SiO_2 glass, which could enable to considerably extend the performance of Ge-based devices above 1300 K. © *2014 AIP Publishing LLC*.
[http://dx.doi.org/10.1063/1.4868721]

Advances in the study of group IV semiconductor nanostructures over the last two decades have demonstrated the great potential of nucleating Si and Ge nanocrystals in silica through a variety of processes, including, for example, ion implantation and laser ablation. In particular, quantum confinement due to size effects allow to obtain strong luminescence signals from both Si and Ge demonstrating the potential of such systems for luminescent devices and displays.[1–3]

The large thermal diffusivity and high photosensitivity of Ge nanocrystals embedded in silicon oxide glass allow to design nanostructured and monolithically integrated materials that can be used in applications such as third generation solar cells and high-sensitivity optical sensors.[4–7] In addition, UV exposure techniques can be exploited to imprint specific patterns to design and develop advanced optical components, such as Fiber Bragg Gratings (FBGs).[8,9]

These two remarkable properties allow to synthesize Ge nanocrystals by thermal activation, with dimensions that can be controlled by tuning the thermal annealing parameters.[10,11] However, the high mobility of Ge atoms in silicon oxide substrates[12] requires reaching a critical temperature, which leads to poor thermal stability and strong desorption effects above the melting point of bulk Ge (1211 K). Both these effects limit the operating temperature range of Ge-based devices.

The introduction of excess Si atoms into silicon oxide has recently been proposed as a means of increasing the thermal resistance of these materials,[13,14] by demonstrating that the trapping of Ge diffusing atoms by Si can efficiently delay and/or reduce Ge desorption. Excess Si atoms are introduced by Si^+ ion implantation, with a penetration depth that is function of acceleration voltage.[15] For a standard 300 kV commercial implanter, Stopping Range of Ions in Solids and TRansport of Ions in Matter (SRIM-TRIM) simulations indicate that the maximum path of Si^+ ions within silicon oxide cannot exceed 700 nm,[15] thus restricting ion implantation to the treatment of thin films, of the order of half a micron.

It has been also shown that a change in silicon oxidation state could explain the wide range of values of Ge diffusivity in SiO_2 found in the literature, which reports discrepancies of several orders of magnitudes.[12,16–18] This may suggest that Si dangling bonds can affect the diffusion mechanism, by acting as intrinsic traps for Ge atoms.

In this Letter, we study the influence of unsaturated SiO_x chemical bonds in different silicon oxide environments and investigate the effects of the silicon oxide substrate on Ge thermal diffusion. To this end, we use scanning electron microscopy (SEM) imaging of Ge nanocrystals (Ge-ncs) formed in fused silica or silicon oxide thermally grown on a Si substrate and compare the remaining Ge concentration and profiles measured by Rutherford backscattering spectrometry (RBS) in each sample. We show that the observed variations of Ge retention result from a significant change in Ge thermal diffusivity, similar to that reported in mixed Si/Ge systems.[14] Using x-ray photoelectron spectroscopy (XPS), we associate this feature to the trapping of Ge diffusing atoms by Si dangling bonds, whose amount corresponds to the concentration of remaining Ge measured by RBS inside each oxide matrix. Such a scenario is compatible with our previous work on Ge-based materials,[10,13,14] while the increase of Si dangling bonds after implantation is in agreement with the damaging rate induced by ion bombardment in these systems, predicted by Monte-Carlo calculations.[15]

We investigated two different types of silicon oxide matrices commonly employed in the SOI technology: commercial fused silica slices and SiO_2 layers of 300 nm thickness thermally grown by dry oxidation of (100) silicon wafers, performed at 1370 K under ultrapure oxygen flux. ^{74}Ge ions were implanted using a 70 keV ion beam with ion

 © 2014 AIP Publishing LLC

This article is copyrighted as indicated in the article. Reuse of AIP content is subject to the terms at: http://scitation.aip.org/termsconditions. Downloaded to IP: 207.162.24.152 On: Mon, 17 Mar 2014 16:19:51

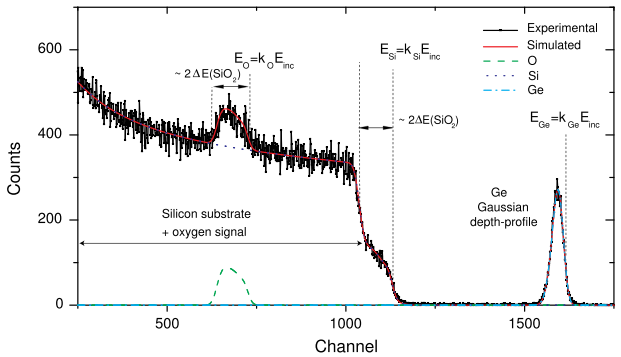

FIG. 1. Example of RBS analysis using SIMTarget, obtained in a SiO_2/Si sample having an oxide layer of 200 nm thickness, implanted with $^{74}Ge+$ ions of 70 keV at a fluence of 8×10^{16} cm^{-2}.

fluences of 4×10^{16} $Ge^+ \cdot cm^{-2}$ and 8×10^{16} $Ge^+ \cdot cm^{-2}$. The implanted samples were then annealed in a quartz tube furnace at 1320 K for 1 h, under an ultra-high purity N_2 atmosphere. SEM cross-section micrographs were recorded from the sample edge using a field emission JEOL JSM7401. A conductive Pt coating was deposited to prevent charge accumulation effects, thus limiting the SEM resolution to the detection of objects greater than 4 nm.[10] The RBS measurements were carried out using He^+ ions, using either a 350 kV Van de Graaff accelerator or a 2 MeV Tandetron. The RBS spectra deconvolution was performed using the SIMNRA[19] and SIMTarget[20] simulation softwares. An example of RBS spectra analysis is presented in Figure 1, showing the different spectral contributions of each atom element found within the target. Both the nature and the fraction of Si chemical bonds were determined by XPS measurements within the first 10 nm of each silicon oxide surface, using a MgK_α (1253.6 eV) monochromatic source focused on a sample surface of about 0.5×0.5 mm^2. The spectra deconvolution was performed using the CasaXPS software, where the energy of all observed peaks was calibrated from the C1s binding energy of 284.6 eV.

Figure 2 shows the effects of different silicon oxide substrates on both the synthesis of Ge-ncs and the Ge desorption after thermal annealing at 1320 K for 1 h. Figure 2(a) refers to a fused silica sample, and Fig. 2(c), to a thin thermal oxide layer grown on a Si wafer (SiO_2/Si). These two samples were implanted and annealed under identical conditions. For each sample, high resolution SEM micrographs allow to identify the grown nanocrystals, whose crystallinity has been demonstrated by x-ray diffraction and Raman measurements.[10] The Ge depth-profile associated with Ge-ncs is measured by RBS analysis, before and after thermal annealing. The distribution of implanted Ge ions is calculated using the SRIM-TRIM code,[15] taking into account ion sputtering effects. It is presented in Figures 2(a) and 2(c) to indicate the maximum depth range of 90 nm (indicated by a yellow arrow) at which Ge ions have been introduced into the target. The sample surface exposed to Ge ions is marked by the red arrow. Within the first 70–80 nm of both samples, dark and bright nanostructures are observed.

The dark and bright objects are attributed to nanocavities and Ge nanocrystals, respectively.[10] The greater concentration of nanocavities observed in the fused silica sample (Fig. 2(a)) is consistent with the lower concentration of Ge detected by RBS after thermal annealing (Fig. 2(b)). Before annealing, the total surface density of Ge detected in each sample is $7.9 \pm 0.1 \times 10^{16}$ cm^{-2}, whereas after annealing, the concentration of Ge remaining in each sample is $2.8 \pm 0.1 \times 10^{16}$ cm^{-2} and $6.1 \pm 0.2 \times 10^{16}$ cm^{-2}, in fused

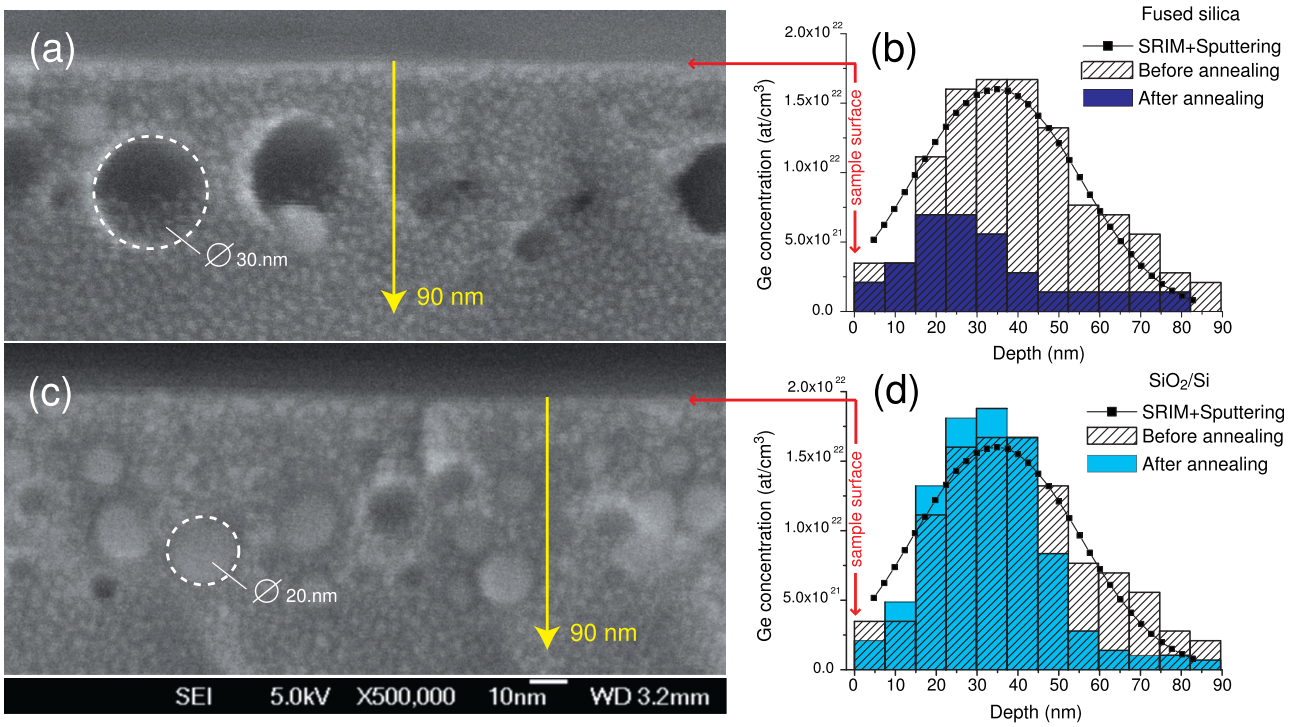

FIG. 2. Cross-section SEM pictures of silica (a) and thermal oxide substrate (c) implanted with 8×10^{16} Ge^+ ions$\cdot cm^{-2}$ and annealed at 1320 K for 1 h, with their respective Ge depth-profiles (b) and (d) measured by RBS before and after thermal treatment.

This article is copyrighted as indicated in the article. Reuse of AIP content is subject to the terms at: http://scitation.aip.org/termsconditions. Downloaded to IP: 207.162.24.152 On: Mon, 17 Mar 2014 16:19:51

silica and SiO_2/Si, respectively. Thus, approximately 65% of the Ge nominally implanted into the fused silica matrix has left the material during thermal treatment, as opposed to only about 25% for SiO_2/Si. In this thermal oxide substrate, the comparison of RBS measurements in Fig. 2(d) also indicates that the shape of the Ge depth-profile after thermal annealing is similar to the one determined immediately after ion implantation. However, although the number of observed nanoparticles is greater in SiO_2/Si (Fig. 2(c)), their sizes are approximately two times smaller than in the case of nanoscale objects observed in fused silica (Fig. 2(a)).

An extensive analysis of SEM micrographs shows that the hundred "objects" we detect within a sample section one micron in width have average diameters of 17.4 ± 2.4 nm and 9.3 ± 1.2 nm, in fused silica and SiO_2/Si, respectively. Comparing the quantity of Ge detected by RBS and the amount of Ge that can be contained within the volume of all nano-objects observed by SEM (bright and dark objects) provides information on the rate of clustering.[10] In a fused silica substrate, the excess Ge occupies a volume less than half that of the nano-objects observed by SEM (Fig. 2(a)), which corresponds approximately to the volume of all Ge ions implanted into the substrate. This suggests that the Ge ions implanted into fused silica have clustered within the first minutes of annealing, before desorption.[10] On the other hand, the amount of Ge that can be contained inside the nano-objects observed in Fig. 2(c) is estimated at approximately $5.8 \times 10^{16}\,cm^{-2}$, indicating that only about 91% of the Ge remaining in the thermal oxide participates in the formation of the observed nanoparticles. The remaining Ge is contained within structures with dimensions smaller than the SEM detection limit or diluted within the oxide.

These observations indicate that the differences in Ge concentration reported for these two different oxide matrices result from significant changes in the Ge thermal diffusivity. The diffusion mechanism involved in both the nucleation of Ge-ncs and Ge desorption is less effective in SiO_2/Si than in fused silica. This trend is also systematically observed (not shown) for samples of SiO_2 thickness varying between 100 and 2000 nm, thermally grown on Si wafers doped with different elements (B, P, As), and annealed at temperatures higher than 1220 K (up to 1420 K) for 30 and 60 min. Nevertheless, precise measurements by RBS of the Si/O fraction in SiO_2/Si and fused silica substrates (not shown) do not allow us to detect significant changes of their oxygen stoichiometry using this experimental approach.

The XPS analysis of the Si2p peak, measured in pristine fused silica (Fig. 3(a)) and thermal oxide (Fig. 3(b)) substrates is presented in Fig. 3. The spectra are deconvoluted for both $2p_{3/2}$ and $2p_{1/2}$ electron levels using the method described in Ref. 21, for energy values reported with respect to the bulk Si state. Two different spectral contributions are identified, each centered at energy positions of -3.9 eV and -2.4 eV, identical to the values typical of a SiO_2/Si interface.[21] The first peak is associated with photoelectrons originating from Si atoms in complete oxidation state (Si^{4+}), whose four valence electrons are bonded to oxygen atoms. The second peak corresponds to Si atoms (Si^{3+}) having three oxygen chemical bonds with one remaining free valence electron. The ratio of the integrated intensity of these

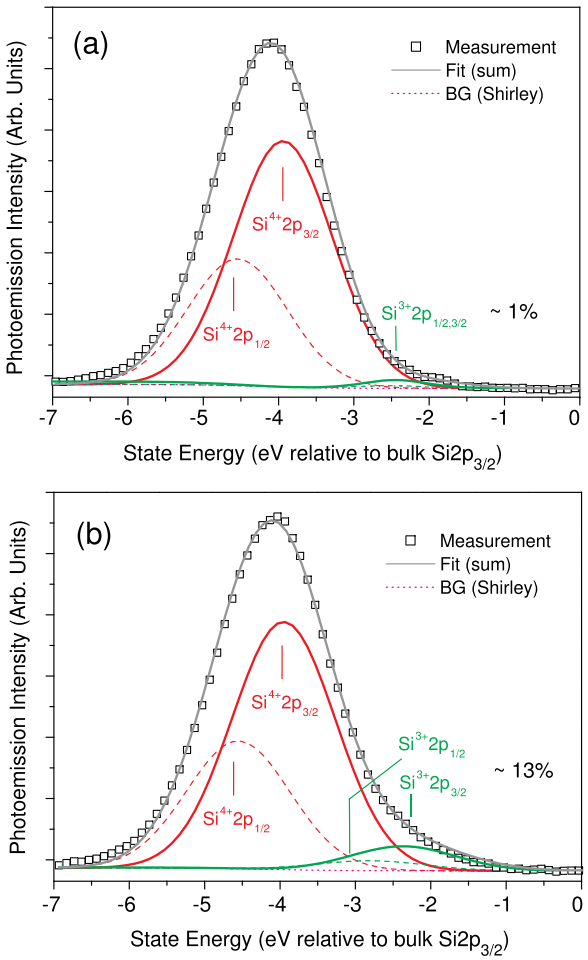

FIG. 3. Spectral analysis of Si^{4+}2p and Si^{3+}2p peaks measured by XPS in virgin fused silica (a) and SiO_2/Si (b) substrates.

spectral contributions provides relative fractions of silicon dangling bonds of $\sim 1\% \pm 1\%$ in fused silica, and $\sim 13\% \pm 2\%$ in thermal silicon oxide. To verify that such a difference persists after ion bombardment, we also measured the fraction of Si atoms remaining in complete oxidation state, right after exposing each substrate to a Ge^+ ion beam (and before thermal annealing). Previous studies of implanted materials have shown that the damage induced by ion implantation is usually responsible for breaking a high number of O-Si-O bonds within the oxide, proportionally to the quantity of impinging ions (neglecting ion sputtering effects).[22] Since the damaging increases with the atomic mass of ion species,[15] this can lead to the possible elimination of all Si atoms in complete oxidation state. Such a degradation of the silicon chemical bonds is not observed for ion fluences of $4 \times 10^{16}\,cm^{-2}$ or of $8 \times 10^{16}\,cm^{-2}$, since we obtain fractions of Si^{4+} chemical bonds around $70\% \pm 2\%$ and $84\% \pm 2\%$ in SiO_2/Si and fused silica samples, respectively. The difference between the relative intensity of Si^{4+}2p and Si^{3+}2p peaks also indicates that after ion implantation, there is still approximately 13%–14% more Si bonded with four oxygen atoms in fused silica, than in SiO_2/Si. Due to the trapping efficiency of Si-Ge chemical bonds,[14] we infer that such an increase of Si dangling bonds is related to greater Ge retention in SiO_2/Si. On the other hand, we

This article is copyrighted as indicated in the article. Reuse of AIP content is subject to the terms at: http://scitation.aip.org/termsconditions. Downloaded to IP: 207.162.24.152 On: Mon, 17 Mar 2014 16:19:51

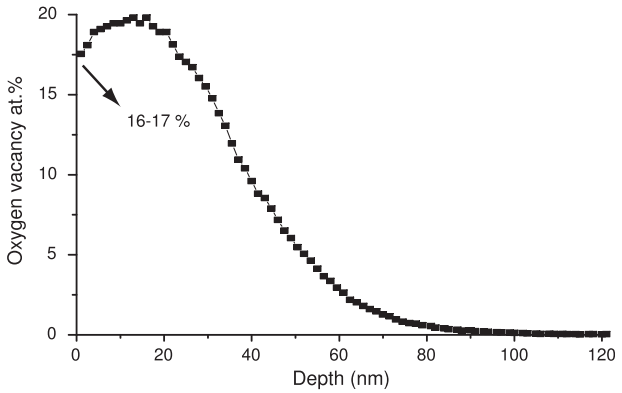

FIG. 4. Depth-distribution of oxygen vacancies (including sputtering effects), generated by Ge^+ impinging ions of 70 keV into SiO_2, for a fluence of $4 \times 10^{16}\,cm^{-2}$. The concentrations are given in at. % with respect to the target oxygen density.

observe that the fraction of Si in intermediate oxygen state increases by $\sim 15\%$ after ion bombardment in both substrates. This value is consistent with the density of oxygen vacancies generated by impinging ions we present in Figure 4, whose relative atom concentration is evaluated at approximately 16%–17% according to SRIM calculations.[15]

Using the discrepancy between the concentrations of Si dangling bonds in different substrates measured by XPS, we can evaluate the additional number of Ge atoms that could be trapped by the Si partially bonded with O inside SiO_2/Si during annealing. By assuming that the mobility of Si atoms in silicon oxide can be neglected at a temperature of 1320 K,[18] the surface density of Ge atoms held by Si dangling bonds can be estimated by

$$N_{Ge} = N_{Si^*} \times \tau_{Si}, \quad (1)$$

where N_{Si*} is the surface density of Si atoms having one dangling bond and τ_{Si} is the average trapping rate of diffusing Ge by Si. The surface density of Si is $2.05 \times 10^{17}\,cm^{-2}$ within the first 90 nm of the SiO_2/Si sample, so that $N_{Si*} = 2.70 \times 10^{16}\,cm^{-2}$ according to XPS results. The average trapping rate (τ_{Si}) of Ge diffusing atoms by excess Si during annealing of 1 h at 1320 K (see the slope of the lines presented in the Fig. 1 of Ref. 14) is estimated at $\tau_{Si} = 0.99$, giving $N_{Ge} = 2.6 \pm 0.4 \times 10^{16}\,cm^{-2}$. This amount of Ge that can be potentially retained by Si dangling bonds is close to the difference of $3.3 \pm 0.3 \times 10^{16}\,cm^{-2}$ we measured by RBS between the surface densities of Ge in SiO_2/Si and fused silica (Figs. 2(b) and 2(d)). This indicates that the results obtained by XPS on the relative concentration of Si dangling bonds are both qualitatively and quantitatively consistent with SEM and RBS measurements. As for the silicon excess introduced by co-implantation,[13,14] silicon dangling bonds inside a silicon oxide substrate can reduce Ge mobility by trapping Ge diffusing atoms under high temperature annealing. We conclude that the greater concentration of Ge remaining in SiO_2/Si samples is compatible with a diffusion mechanism which involves the participation of a concentration of 13% of Si dangling bonds within this material, while their effect is negligible in fused silica.

In addition to the role of silicon in the formation mechanism of Ge-ncs,[16] this makes the reduction of silicon oxidation states in silica glass interesting for improving the operating range of Ge-based devices and sensors in high temperature environment. To promote and monitor the breaking of Si-O chemical bonds in specific regions, different scenarios could be investigated, such as the growth or the deposition of non-stoichiometric SiO_x, the exposure of silica substrates to energetic lasers, as well as high-energy light-ion implantations, using H^+ and He^+, whose penetration depths can be 10 times greater than for Si^+ ions implanted at the same energy.[15]

In summary, we have shown that there exists a marked difference of the Ge thermal diffusion and desorption in substrates of silicon oxide thermally grown on Si and fused silica. These features can be explained by the presence of a greater concentration of Si dangling bonds in SiO_2/Si, which hinder desorption by trapping Ge atoms and increase their stability inside the oxide matrix by annealing above 1300 K for 1 h. From simple calculations, we have shown that the concentrations of Si dangling bonds measured in each sample can be directly related with the concentration of remaining Ge. Thus, the control of Si atoms having an intermediate oxidation state in silicon oxide can be a promising technique for improving the thermal resistance of Ge-based glass, with potentially important implications for device performance in harsh environments, such as car/airplane engines, space and nuclear reactors.

This work was supported by the Québec-Wallonie-Bruxelles collaboration ST-4/07.801 and the NSERC Strategic Grant STPGP 447377-13 in partnership with MPB. The authors would like to thank C. Chabanier and S. Delprat for technical assistance. F.R. acknowledges partial salary support from the Canada Research Chairs program. Y. Q. Wang would like to thank financial support from the Natural Science Foundation for Outstanding Young Scientists in Shandong Province (Grant No. JQ201002) and the Taishan Outstanding Overseas Scholar Program of Shandong Province.

[1]L. T. Canham, Appl. Phys. Lett. **57**, 1046 (1990).
[2]Z. H. Lu, D. J. Lookwood, and J.-M. Baribeau, Nature **378**, 258 (1995).
[3]L. Pavesi, L. Dal Negro, C. Mazzoleni, G. Franzo, and F. Priolo, Nature **408**, 440 (2000).
[4]S. Ossicini, M. Amato, R. Guerra, M. Palummo, and O. Pulci, Nanoscale Res. Lett. **5**(10), 1637 (2010).
[5]A. Gillooly, Nat. Photonics **5**, 468 (2011).
[6]D. Riabinina, C. Durand, F. Rosei, and M. Chaker, Phys. Status Solidi A **204**, 1623 (2007).
[7]L. Nikolova, T. B. LaGrange, B. W. Reed, M. J. Stern, N. D. Browning, G. H. Campbell, J.-C. Kieffer, B. J. Siwick, and F. Rosei, Appl. Phys. Lett. **97**, 203102 (2010).
[8]*Fiber Optics Sensors: An introduction for Engineers and Scientists*, 2nd ed., edited by E. Udd (Wiley-Interscience, New York, NY, 2006).
[9]A. Gusarov, S. Vasiliev, O. Medvedkov, I. Mckenzie, and F. Berghmans, IEEE Trans. Nucl. Sci. **55**, 2205 (2008).
[10]D. Barba, F. Martin, J. Demarche, G. Terwagne, and G. G. Ross, Nanotechnology **23**, 145701 (2012).
[11]D. Riabinina, C. Durand, M. Chaker, N. Rowell, and F. Rosei, Nanotechnology **17**, 2152 (2006).
[12]A. Markwitz, B. Schmidt, W. Matz, R. Grötzschel, and A. Mücklig, Nucl. Instrum. Methods Phys. Res., Sect. B **142**, 338 (1998).
[13]D. Barba, F. Martin, J. Demarche, G. Terwagne, and G. G. Ross, Appl. Phys. Lett. **101**, 143107 (2012).
[14]D. Barba, F. Martin, J. Demarche, G. Terwagne, and G. G. Ross, J. Appl. Phys. **114**, 074306 (2013).

This article is copyrighted as indicated in the article. Reuse of AIP content is subject to the terms at: http://scitation.aip.org/termsconditions. Downloaded to IP: 207.162.24.152 On: Mon, 17 Mar 2014 16:19:51

[15]J. F. Ziegler, M. D. Ziegler, and J. P. Biersack, Nucl. Instrum. Methods Phys. Res., Sect. B **268**, 1818 (2010).
[16]D. Yu and G. S. Hwang, Electrochem. Solid-State Lett. **11**(12), P17 (2008).
[17]V. Beyer and J. von Borany, Phys. Rev. B **77**, 014107 (2008).
[18]M. V. Minke and K. A. Jackson, J. Non-Cryst. Solids **351**, 2310 (2005).
[19]M. Mayer, "SIMNRA User's Guide," Report No. IPP 9/113, Max-Planck Institut für Plasmaphysik, Garching, Germany, 1997.
[20]J. L. Colaux, T. Thome, and G. Terwagne, Nucl. Instrum. Methods Phys. Res., Sect. B **254**, 25 (2007). SimTarget code is available from: http://www.namur.be/simtarget.
[21]F. J. Himpsel, F. R. McFeely, A. Taleb-Ibrahimi, and J. A. Yarmoff, Phys. Rev. B **38**(9), 6084 (1988).
[22]D. Barba, D. Koshel, F. Martin, G. G. Ross, M. Chicoine, F. Schiettekatte, M. Yedji, J. Demarche, and G. Terwagne, J. Lumin. **130**, 669 (2010).

This article is copyrighted as indicated in the article. Reuse of AIP content is subject to the terms at: http://scitation.aip.org/termsconditions. Downloaded to IP: 207.162.24.152 On: Mon, 17 Mar 2014 16:19:51